Materials Research Letters

ISSN: (Print) (Online) Journal homepage: https://www.tandfonline.com/loi/tmrl20

Investigation of sluggish diffusion in FCC $Al_{0.25}CoCrFeNi$ high-entropy alloy

Abhishek Mehta & Yongho Sohn

To cite this article: Abhishek Mehta & Yongho Sohn (2021) Investigation of sluggish diffusion in FCC $Al_{0.25}CoCrFeNi$ high-entropy alloy, Materials Research Letters, 9:5, 239-246, DOI: 10.1080/21663831.2021.1878475

To link to this article: https://doi.org/10.1080/21663831.2021.1878475

MATER. RES. LETT.
2021, VOL. 9, NO. 5, 239–246
https://doi.org/10.1080/21663831.2021.1878475

MATERIALS RESEARCH LETTERS
Taylor & Francis
Taylor & Francis Group

ORIGINAL REPORT

Investigation of sluggish diffusion in FCC $Al_{0.25}CoCrFeNi$ high-entropy alloy

Abhishek Mehta and Yongho Sohn

Department of Materials Science and Engineering, University of Central Florida, Orlando, FL, USA

ABSTRACT

To validate the 'sluggish diffusion' in high-entropy alloys, interdiffusion coefficients of individual elements and tracer diffusion coefficient of Ni were experimentally determined in FCC $Al_{0.25}CoCrFeNi$ alloy. The tracer diffusion coefficient was determined without the application of radio-tracers using a novel analytical method proposed by Belova et al. based on linear response theory coupled with Boltzmann-Matano approach and Gaussian distribution function. Sluggish diffusion kinetics was not observed in alloys with higher configuration entropy in comparison to alloys with lower configuration entropy. Correspondingly, potential energy fluctuations in alloys with higher configuration entropy may not always result in anomalously slow diffusion kinetics.

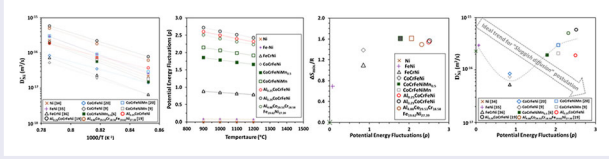

IMPACT STATEMENT

Diffusion is determined not to be necessarily sluggish in $Al_{0.25}CoCrFeNi$ high-entropy alloy by experimental measurement of chemical and tracer diffusion coefficients.

ARTICLE HISTORY
Received 7 December 2020

KEYWORDS
High-entropy alloys; tracer diffusion; interdiffusion; potential energy fluctuations; sluggish diffusion; entropy of mixing

1. Introduction

High-entropy alloys (HEAs) were initially proposed to exhibit *sluggish diffusion* kinetics [1,2], based on the indirect observations, e.g. absence of low-temperature phases upon slow cooling from elevated temperature [3], limited growth of nano-crystals [4,5], etc. Therefore, it was postulated that the formation of a new phase would require a cooperative movement of many different kinds of atoms to accomplish the partitioning in composition, which would be difficult in HEAs in comparison to solvent-based alloys.

The initial investigation by Tsai et al. [6] supported the sluggish diffusion kinetics in $CoCrFeNiMn_{0.5}$ alloy by estimating the tracer diffusion coefficients using the interdiffusion data. However, the following work by Vaidya and coworkers [7–9] on CoCrFeNi and CoCrFeNiMn alloys suggested that diffusion may be slow at an inverse homologous temperature but not at absolute temperatures. Other experimental investigations [10–13] also suggested that sluggish diffusion kinetics may not be true in CoCrFeNi and CoCrFeNiMn HEAs. Few interdiffusion investigations [14] supported the sluggish diffusion effects, while others [15–19] suggest that the sluggish diffusion effect cannot be generalized for all HEAs.

Direct experimental measurement of tracer diffusion coefficients was previously performed in CoCrFeNi and CoCrFeNiMn alloys [9] and experimental measurement of interdiffusion coefficient was performed in CoFeMnNi [17], CoCrMnNi [17], CoCrFeNi [20], CoCrFeNiMn [20], AlCoCrFeNi [15], AlCoCrFeNiMn [16], CoCrCuFeNi [21], AlCoCrFeTiNi [22] alloys. Few other investigations had either numerically estimated the tracer diffusion coefficients using interdiffusion data, for example in Al-Co-Cr-Fe-Ni [14,19], Co-Fe-Mn-Ni [17], Co-Cr-Mn-Ni [17], Co-Cr-Cu-Fe-Ni [21], Al-Co-Cr-Fe-Ti-Ni [22] alloy, or suggested that intrinsic diffusion coefficient is similar to tracer diffusion coefficient based on ideal solution behavior in $CoCrFeNiMn_{0.5}$ alloy [6]. Recent

CONTACT Abhishek Mehta abhi@knights.ucf.edu Department of Materials Science and Engineering, University of Central Florida, 12760 Pegasus Drive, Orlando, FL 32816, USA

Supplemental data for this article can be accessed here. https://doi.org/10.1080/21663831.2021.1878475

review articles [23,24] comprehensively summarizes all the interdiffusion and tracer diffusion investigations performed in HEAs.

In this study, both interdiffusion and tracer diffusion coefficients were experimentally determined in FCC $Al_{0.25}CoCrFeNi$ alloy. Interdiffusion coefficients were determined for individual elements using traditional diffusion couple approach using Dayananda-Sohn approach [25] in the temperature range from 900°C to 1200°C. Tracer diffusion coefficient of Ni in $Al_{0.25}CoCrFeNi$ alloy was determined, without the use of radioactive tracers, using a sandwich diffusion couple experiment, where concentration profiles are analyzed by a novel formalism, established by Belova et al. [26], based on linear response theory coupled with Boltzmann-Matano approach and Gaussian distribution function [26,27]. Then, tracer diffusivity of Ni (D^*_{Ni}) was compared with the diffusivities in other FCC alloys with varying configurational entropy of mixing (ΔS_{mix}) and corresponding potential energy fluctuations (PEF). Analytical emphasis was given to examine any correlation between D^*_{Ni}, ΔS_{mix}, and PEF to examine the sluggish diffusion postulation in HEA.

2. Materials and method

Single-phase composition of FCC $Al_6Co_{19}Cr_{28}Fe_{28}Ni_{19}$ and $Al_6Co_{28}Cr_{19}Fe_{19}Ni_{28}$ alloys were arc-melted using elemental Al, Co, Cr, Fe, and Ni with a minimum purity of 99.9%. To ensure the compositional homogeneity, alloys were melted, flipped, and re-melted five times and subsequently homogenized at 1100°C for 48 h in an argon atmosphere, followed by water quenching. For measurement of interdiffusion coefficients, metallographically polished surfaces ($\sim 1\mu$m surface finish) of two alloys were placed in intimate contact in two stainless steel jigs and held tightly by clamping screws. Details on diffusion couple fabrication for the determination of interdiffusion coefficients have been described elsewhere [28–33]. For measurement of tracer diffusion coefficients, an alloy disc polished on both sides was sandwiched between two alloys of the same composition. At one of the interfaces between the two alloys existed a sputter-deposited thin film of pure Ni ($\sim$900 nm thickness). Details on the diffusion couple assembly in sandwich configuration with a thin film to measure the tracer diffusivity also have been reported elsewhere [26,27]. All diffusion couples were isothermally annealed at a predetermined temperature, and subsequently, water quenched. Then, couples were sectioned normal to the diffusion couple interface and metallographically polished down to 1 μm surface finish. The concentration profiles were acquired from the Thermo-Scientific™ X-ray energy dispersive spectroscopy (XEDS) equipped on Zeiss™ Ultra-55 field emission scanning electron microscope (FE-SEM). Experimental concentration profiles measured from XEDS in this study were curve fitted using Origin™ Pro 8.5 software, with non-linear curve fitting function given by [15,27]:

$$c(x) = \frac{p_1 + p_3x + p_5x^2 + p_7x^3}{1 + p_2x + p_4x^2 + p_6x^3} \tag{1}$$

3. Results and analyses

The average effective interdiffusion coefficient can be determined for any component over the desired composition range by [25]:

$$\int_{x_1}^{x_2} \tilde{J}_i dx = -\overline{\tilde{D}}_i^{\text{eff}} (C_i(x_1) - C_i(x_2)) = -\frac{1}{2t} \int_{C_i(x_1)}^{C_i(x_2)} (x - x_o)^2 dC_i (i = 1, 2 \ldots, n) \tag{2}$$

where $\overline{\tilde{D}}_i^{\text{eff}}$ is the average effective interdiffusion coefficient of component i for the composition range, $C_i(x_1)$ to $C_i(x_2)$. The detailed procedure for the determination of $\overline{\tilde{D}}_i^{\text{eff}}$ and limitations of using the Boltzmann-Matano method extended to a multi-component system to determine the main and cross interdiffusion coefficients, specifically for HEAs, have been documented previously by Mehta and Sohn [15,16]. Figure 1(a–d) presents the concentration profiles superimposed on backscatter electron micrographs of $Al_6Co_{19}Cr_{28}Fe_{28}Ni_{19}$ vs. $Al_6Co_{28}Cr_{19}Fe_{19}Ni_{28}$ diffusion couples isothermally annealed at (a) 900°C for 240 h, (b) 1000°C for 120 h, (c) 1100°C for 48 h, and (d) 1200°C for 24 h. Figure 1(e) shows the temperature dependence of $\overline{\tilde{D}}_i^{\text{eff}}$ for Co, Cr, Fe, and Ni. For $Al_{0.25}CoCrFeNi$ alloy, $\overline{\tilde{D}}_{Fe}^{\text{eff}} < \overline{\tilde{D}}_{Ni}^{\text{eff}} < \overline{\tilde{D}}_{Cr}^{\text{eff}} < \overline{\tilde{D}}_{Co}^{\text{eff}}$. The $\overline{\tilde{D}}_{Al}^{\text{eff}}$ remained negative for all temperatures because of the large negative value of off-diagonal interdiffusion coefficients, i.e. strong thermodynamic interaction of Al with other elements (uphill diffusion). Interdiffusion coefficients, activation energy, and pre-exponential factors are reported in Table S1 of *Supplementary Materials*.

Tracer diffusion coefficient can be measured using the analytical formalism proposed by Belova et al. [26]:

$$D^*_A = -\left(\frac{x + a}{2t} - \frac{G_2}{C_{X2}}\right) / \left(\frac{d \ln(c_{X1}/c_{X2})}{dx}\right) \tag{3}$$

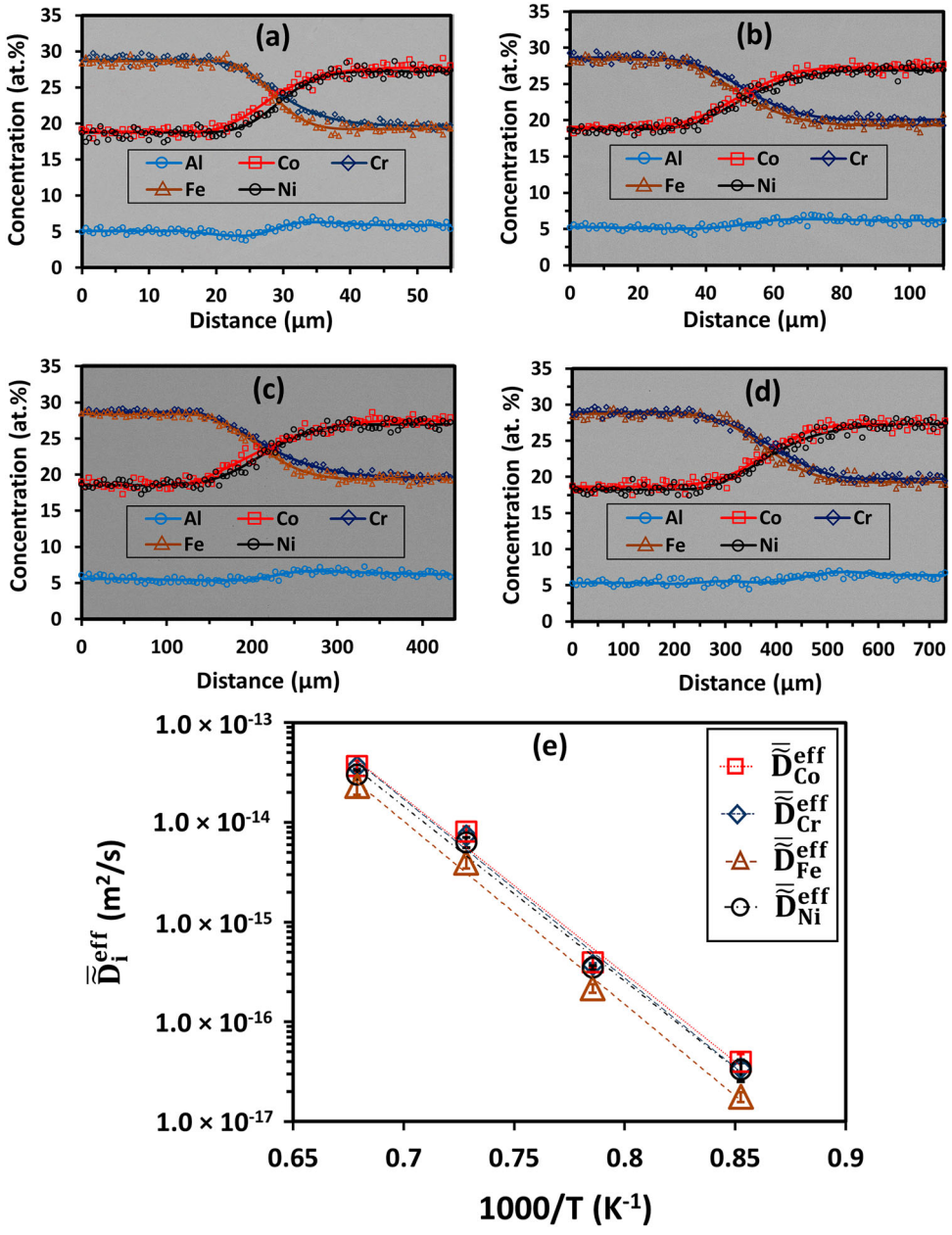

Figure 1. Concentration profiles superimposed on backscatter electron micrographs of $Al_6Co_{19}Cr_{28}Fe_{28}Ni_{19}$ vs. $Al_6Co_{28}Cr_{19}Fe_{19}Ni_{28}$ diffusion couples isothermally annealed at (a) 900°C for 240 h, (b) 1000°C for 120 h, (c) 1100°C for 48 h, and (d) 1200°C for 24 h. (e) Temperature dependence of average effective interdiffusion coefficients ($\tilde{\bar{D}}_i^{\text{eff}}$) for Co, Cr, Fe, and Ni.

where a is a constant and the value of G_2 can be determined using:

$$G_2 = \frac{c_{X2}^{+} - c_{X2}^{-}}{2t} \times \left[(1 - y_{X2}^{*}) \int_{-\infty}^{x^*} y_{X2} dx + y_{X2}^{*} \int_{x^*}^{\infty} (1 - y_{X2}) dx \right] \quad (4)$$

Determination of G_2 and a have been described by Belova et al. [26]. Schulz et al. [27] used this approach to demonstrate that the Gaussian distribution function can be utilized to determine tracer diffusion coefficient using full width at half maxima (FWHM) of the thin film diffusion profile as:

$$D^* = \frac{\text{FWHM}^2}{16 \ln 2 \, t} \quad (5)$$

Figure 2(a) presents the schematics of the sandwich diffusion couple to determine the tracer diffusion coefficient of Ni in $Al_{0.25}CoCrFeNi$. Tracer diffusion coefficients were determined by isothermally annealing the sandwich diffusion couples at 900°C for 12 h, 950°C for 6 h, and

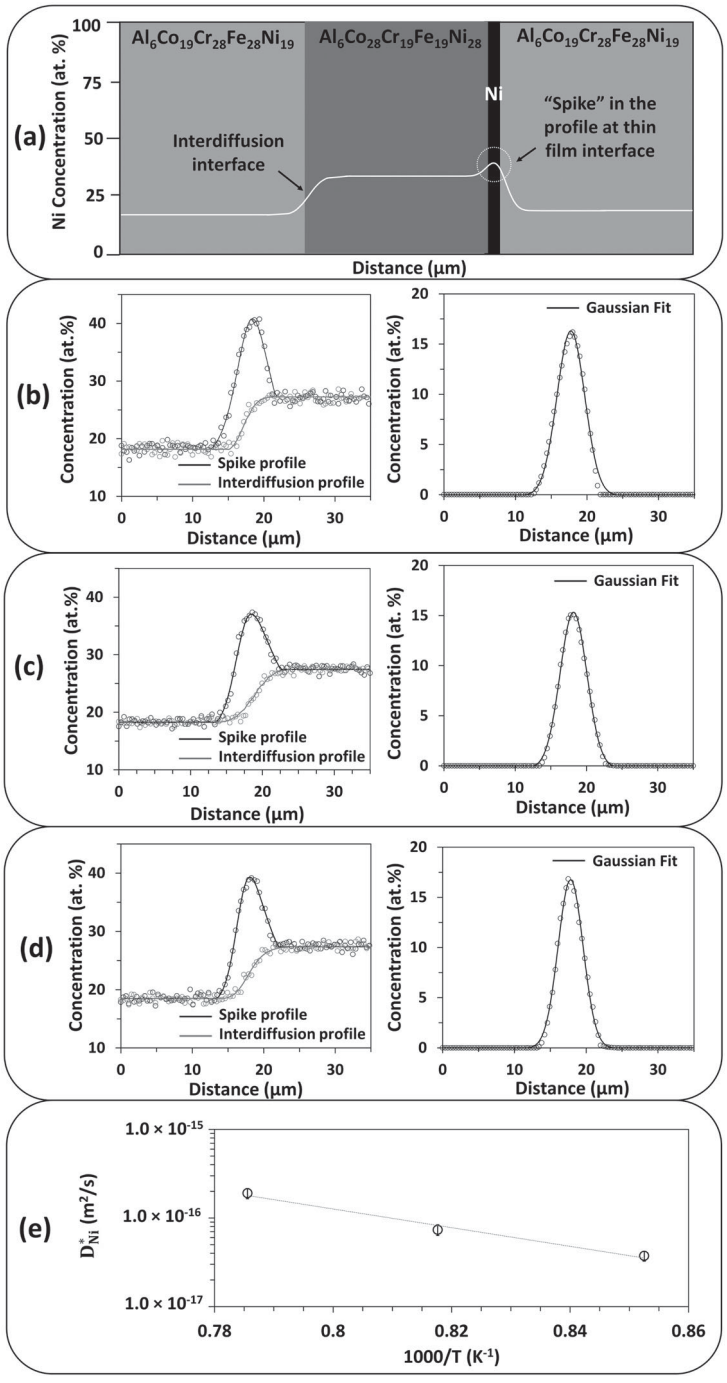

Figure 2. (a) A schematic representation of sandwich diffusion couple assembly utilized to determine the tracer diffusion coefficient of Ni in $Al_{0.25}$CoCrFeNi. Concentration profile of Ni from thin film interface (Spike profile) superimposed on the Concentration profile of Ni from interdiffusion interface (Interdiffusion profile) and corresponding Gaussian fitted concentration profile obtained after mathematical subtraction of interdiffusion concentration profile from spike profile after annealing the sandwich diffusion couple at (b) 900°C for 12 h, (c) 950°C for 6 h, and (d) 1000°C for 2 h. (e) Temperature dependence of the Trace diffusion coefficients of Ni in $Al_{0.25}$CoCrFeNi.

1000°C for 2 h. Figure 2(b–d) shows the concentration profiles of Ni at the interdiffusion interface and thin-film interface (i.e. spike profile) overlaid on each other, and the corresponding Gaussian fitted profile obtained after mathematical subtracting the spike profile from the interdiffusion profile at 900°C, 950°C and 1000°C. Figure 2(e) presents the tracer diffusion coefficient of Ni in $Al_{0.25}$CoCrFeNi HEA for the temperature range, 900–1000°C. Activation energy and pre-exponential factors were determined to be 201.7 kJ/mol and 3.4×10^{-8} m^2/s, respectively. Although, this is the first experimental investigation to measure D^*_{Ni} in $Al_{0.25}$CoCrFeNi,

Table 1. Ni tracer diffusion coefficients in various compositions of Al-Co-Cr-Fe-Ni high-entropy alloys.

	This study	Numerical extrapolation approach [14,19]		
T (K)	$Al_{0.25}$ CoCrFeNi	$Al_pCo_qCr_r$ Fe_sNi_t [14]	$Al_{6.64}Co_{23.82}$ $Cr_{23.66}$ $Fe_{23.01}Ni_{22.87}$ ($\sim Al_{0.29}$ CoCrFeNi) [19]	$Al_{4.88}Co_{29.53}$ $Cr_{18.58}$ $Fe_{19.62}Ni_{27.39}$ [19]
1173	3.7×10^{-17}	1.3×10^{-17}	7.9×10^{-17}	6.2×10^{-17}
1223	7.4×10^{-17}	3.4×10^{-17}	2.2×10^{-17}	1.8×10^{-16}
1273	1.9×10^{-16}	1.0×10^{-16}	5.9×10^{-16}	5.0×10^{-16}

however, Li et al. [19] and Dabrowa et al. [14] had previously estimated the D^*_{Ni} in FCC $Al_{0.29}$CoCrFeNi and FCC off-equiatomic $Al_pCo_qCr_rFe_sNi_t$ alloys, respectively, using the numerical extrapolation of interdiffusion data. Table 1 reports the D^*_{Ni} in various Al-Co-Cr-Fe-Ni alloys, and suggest that D^*_{Ni} is lowest in off-equiatomic $Al_pCo_qCr_rFe_sNi_t$ alloy. Moreover, D^*_{Ni} is slightly higher in $Al_{0.29}$CoCrFeNi (i.e. lower configurational entropy) than $Al_{0.25}$CoCrFeNi which contradicts the sluggish diffusion hypothesis.

4. Discussion

Figure 3 compares the interdiffusion coefficients of individual elements in CoCrFeNi [20], CoCrFeNiMn [20], AlCoCrFeNi [15], and AlCoCrFeNiMn [16] FCC alloys. The $\tilde{\overline{D}}^{eff}_{Co}$, $\tilde{\overline{D}}^{eff}_{Cr}$, and $\tilde{\overline{D}}^{eff}_{Ni}$ is the lowest in CoCrFeNi quaternary alloy. The $\tilde{\overline{D}}^{eff}_{Al}$ is lower in quinary $Al_pCo_qCr_rFe_sNi_t$ than in $Al_pCo_qCr_rFe_sNi_tMn_u$. The $\tilde{\overline{D}}^{eff}_{Mn}$ is similar in CoCrFeNiMn and $Al_pCo_qCr_rFe_sNi_tMn_u$ alloys. *Generally, interdiffusion coefficients are not always lower in alloys with a composition corresponding to a higher configurational entropy of mixing.* Figure 4 compares the tracer diffusion coefficient of Ni in Ni [34], FeNi [35], FeCrNi [36], CoCrFeNi [9,20], CoCrFeNiMn [6,9,20], AlCoCrFeNi [19] FCC alloys. Based on the sluggish diffusion effect, the self-diffusion of Ni should be the fastest and the tracer diffusion coefficient of Ni in CoCrFeNiMn should be the slowest. However, D^*_{Ni} is the highest in $Al_{0.29}$CoCrFeNi alloy, and the lowest in quaternary CoCrFeNi. *In general, a decrease in tracer diffusion*

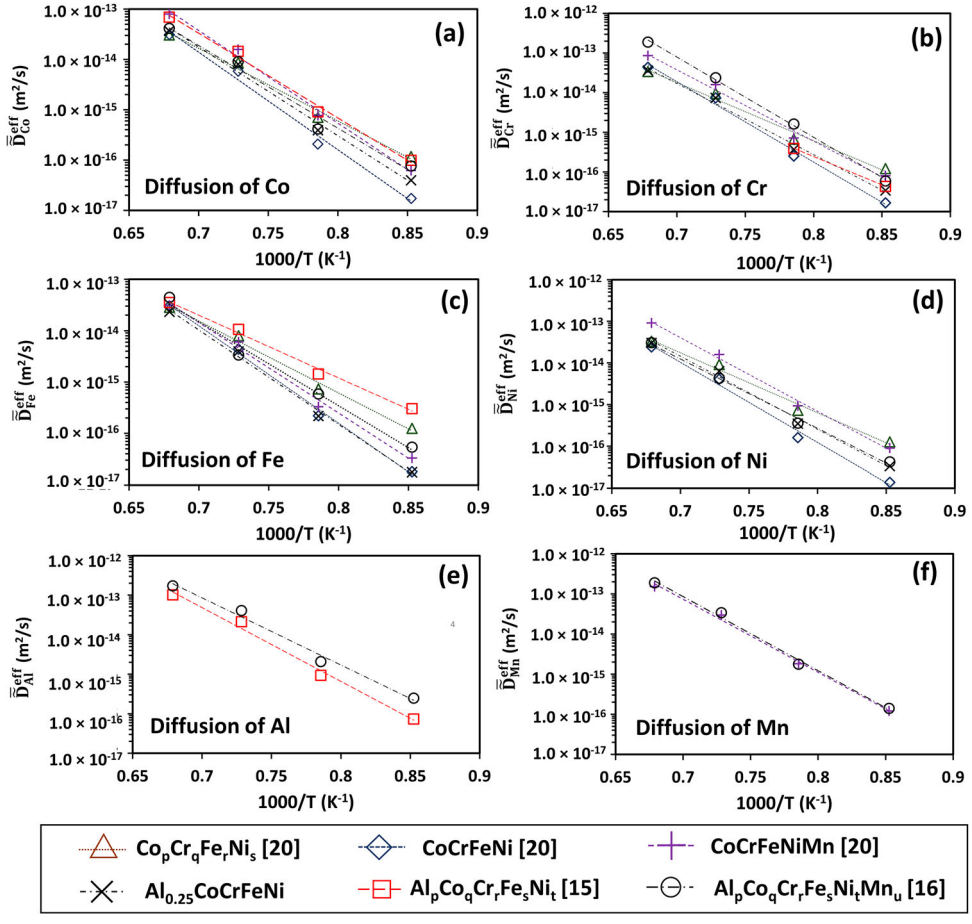

Figure 3. Average effective interdiffusion coefficients of (a) Co, (b) Cr, (c) Fe, (d) Ni, (e) Al, and (f) Mn in various FCC alloys as a function of temperature.

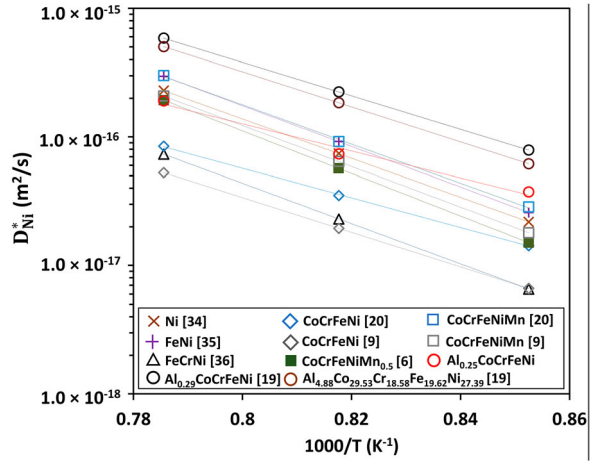

Figure 4. Tracer diffusion coefficient of Ni (D^*_{Ni}) in various FCC alloys as a function of temperature.

coefficient of Ni was not observed in alloys with an increase in number of elements in an alloy system.

It was postulated that in HEAs each atom has a different neighboring atom, therefore an atom experiences a mismatch in atomic size and difference in bond strength which give rise to fluctuation in lattice potential energy [6]. These Potential energy fluctuations (PEF) in the potential energy landscape of the lattice sites is one of the important parameters which may contribute towards the creation of highly stable low energy sites, which can act as atomic traps and results in anomalously slow diffusion kinetics [6]. The PEF normalized to the thermal energy fluctuations ($\sim k_BT$) due to mismatch in atomic size and difference in bond energies of the neighboring atoms in HEAs can be determined using [37]:

$$p = 4.12\delta \times \sqrt{\frac{\bar{K}\bar{V}}{k_BT}} + 2\sqrt{\frac{\sqrt{\sum_i \sum_{j,i\neq j} X_i X_j (\Delta H_{ij}^{mix} - \bar{H})^2}}{k_BT}} \quad (6)$$

where δ $\left(=\sqrt{\sum_{i=1}^{n} X_i\left(1-\frac{r_i}{\sum^{X_i} r_i}\right)^2}\right)$ represents the mismatch in atomic size, X_i is the composition of constituent elements, r_i is the atomic radius, $\bar{K}$ is the composition-weighted average bulk modulus, $\bar{V}$ is the composition-weighted average atomic volume, and ΔH_{ij}^{mix} is the binary pair enthalpy of mixing of the constituents elements determined using Miedema's macroscopic model [38]. Figure 5(a) shows the temperature dependence of the normalized PEF in Ni, FeNi, FeCrNi, CoCrFeNi, CoCrFeNiMn and AlCoCrFeNi alloys. For a given alloy composition, normalized PEF (p) decreased with an increase in temperature, and varied as: p(Ni) < p(FeNi) < p(FeCrNi) ≈ p(CoCrFeNi) < p(CoCrFeNiMn$_{0.5}$) < p(CoCrFeNiMn) < p(Al$_{4.88}$Co$_{29.53}$Cr$_{18.58}$Fe$_{19.62}$Ni$_{17.39}$) < p(Al$_{0.25}$CoCrFeNi) < p(Al$_{0.29}$CoCrFeNi). The entropy of mixing (ΔS) in these alloys varied as: ΔS(Ni) < ΔS(FeNi) < ΔS(FeCrNi) < ΔS(CoCrFeNi) < ΔS(Al$_{4.88}$Co$_{29.53}$Cr$_{18.58}$Fe$_{19.62}$Ni$_{27.39}$) < ΔS(Al$_{0.25}$CoCrFeNi) < ΔS(Al$_{0.29}$CoCrFeNi) < ΔS(CoCrFeNiMn$_{0.5}$) < ΔS(CoCrFeNiMn). Therefore, the assumption that PEF increases with an increase in the entropy of mixing, was not true for these alloys. The PEF cannot be directly correlated with entropy of mixing. In fact, PEF in an alloy system is a composition dependent. An addition of new element (e.g. Al or Mn) in an alloy (e.g. CoCrFeNi HEA) with a larger magnitude of the binary pair enthalpy of mixing (ΔH_{ij}^{mix}) with other elements would yield a larger PEF, e.g. p(AlCoCrFeNi) > p(CoCrFeNiMn) because $\Delta H_{Al-X}^{mix} > \Delta H_{Mn-X}^{mix}$ (X = Co, Cr, Fe, Ni) [16], as shown in Table S2 of *Supplementary Materials*.

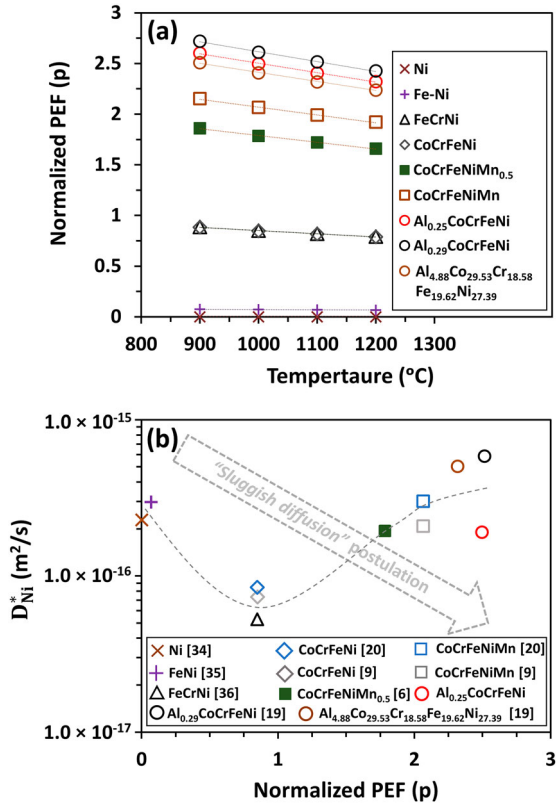

Figure 5. (a) Normalized potential energy fluctuation (p) as a function of temperature and (b) Ni tracer diffusion coefficient as a function normalized potential energy fluctuation (p) at 1000°C for Ni, FeNi, FeCrNi, CoCrFeNi, CoCrFeNiMn$_{0.5}$, CoCrFeNiMn, Al$_{0.25}$CoCrFeNi, Al$_{0.29}$CoCrFeNi, and Al$_{4.88}$Co$_{29.53}$Cr$_{18.58}$Fe$_{19.62}$Ni$_{27.39}$ alloys.

Moreover, the foundation of sluggish diffusion postulation based on PEF theory should yield an inverse relation between tracer diffusivity and PEF. Figure 5(b) shows the D^*_{Ni} determined in this study as a function of PEF at 1000°C. An inverse relationship was not observed

between D^*_{Ni} and PEF, which contradicts the *sluggish diffusion* postulation. Rather, the diffusivity of an element in HEAs appears to be composition-dependent, which suggests the importance of vacancy formation/migration. In the substitutional diffusion mechanism, the lower activation energy required for the vacancy formation and migration would result in faster diffusion kinetics [39]. Furthermore, the magnitude of normalized PEF does not provide any idea about the number of 'atomic traps'. If an alloy exhibit larger PEF and larger D^*_{Ni}, then it would suggest that the number of atomic traps were not sufficient enough to significantly demobilize the diffusing atoms. Finally, the magnitude of PEF in an alloy system also does not provide any idea about the mobility of the vacancies, which is more important in vacancy-mediated diffusion.

5. Conclusions

Interdiffusion coefficients of individual elements and tracer diffusion coefficient of Ni were determined for $Al_{0.25}CoCrFeNi$ high-entropy alloy, and their magnitudes were examined and compared to relevant FCC alloys. Experimental results and related analyses suggest that: (1) diffusivities cannot be correlated with the configurational entropy of mixing; (2) entropy of mixing is not proportional to the potential energy fluctuation exhibited by an alloy system; and (3) no evident correlation between D^*_{Ni} and PEF was observed, therefore, larger magnitude of PEF may not always result in the sluggish diffusion kinetics in HEAs. These findings contradict 'sluggish diffusion' postulation based on configurational entropy of mixing and potential energy fluctuation.

Disclosure statement

No potential conflict of interest was reported by the author(s).

ORCID

Abhishek Mehta http://orcid.org/0000-0003-0884-856X
Yongho Sohn http://orcid.org/0000-0003-3723-4743

References

[1] Yeh JW, Chen SK, Lin SJ, et al. Nanostructured high-entropy alloys with multiple principal elements: novel alloy design concepts and outcomes. Adv Eng Mater. 2004;6(5):299–303.
[2] Yeh JW. Recent progress in high entropy alloys. Ann Chim Sci Mat. 2006;31(6):633–648.
[3] Ng C, Guo S, Luan J, et al. Entropy-driven phase stability and slow diffusion kinetics in an $Al_{0.5}CoCrCuFeNi$ high entropy alloy. Intermetallics. 2012;31:165–172.
[4] Tong CJ, Chen YL, Yeh JW, et al. Microstructure characterization of $Al_xCoCrCuFeNi$ high-entropy alloy system with multiprincipal elements. Metall Mater Trans A. 2005;36(4):881–893.
[5] Chang HW, Huang PK, Yeh JW, et al. Influence of substrate bias, deposition temperature and post-deposition annealing on the structure and properties of multi-principal-component (AlCrMoSiTi)N coatings. Surf Coat Technol. 2008;202(14):3360–3366.
[6] Tsai KY, Tsai MH, Yeh JW. Sluggish diffusion in Co–Cr–Fe–Mn–Ni high-entropy alloys. Acta Mater. 2013;61(13):4887–4897.
[7] Vaidya M, Pradeep KG, Murty BS, et al. Radioactive isotopes reveal a non sluggish kinetics of grain boundary diffusion in high entropy alloys. Sci Rep. 2017;7(1):12293.
[8] Vaidya M, Pradeep KG, Murty BS, et al. Bulk tracer diffusion in CoCrFeNi and CoCrFeMnNi high entropy alloys. Acta Mater. 2018;146:211–224.
[9] Vaidya M, Trubel S, Murty BS, et al. Ni tracer diffusion in CoCrFeNi and CoCrFeMnNi high entropy alloys. J Alloys Compd. 2016;688:994–1001.
[10] Zhang C, Zhang F, Jin K, et al. Understanding of the elemental diffusion behavior in concentrated solid solution alloys. J Phase Equilib Diffus. 2017;38(4):434–444.
[11] Gaertner D, Abrahams K, Kottke J, et al. Concentration-dependent atomic mobilities in FCC CoCrFeMnNi high-entropy alloys. Acta Mater. 2019;166:357–370.
[12] Gaertner D, Kottke J, Wilde G, et al. Tracer diffusion in single crystalline CoCrFeNi and CoCrFeMnNi high entropy alloys. J Mater Res. 2018;33(19):3184–3191.
[13] Kottke J, Laurent-Brocq M, Fareed A, et al. Tracer diffusion in the Ni–CoCrFeMn system: transition from a dilute solid solution to a high entropy alloy. Scr Mater. 2019;159:94–98.
[14] Dąbrowa J, Kucza W, Cieślak G, et al. Interdiffusion in the FCC-structured Al-Co-Cr-Fe-Ni high entropy alloys: experimental studies and numerical simulations. J Alloys Compd. 2016;674:455–462.
[15] Mehta A, Sohn YH. Interdiffusion, solubility limit, and role of entropy in FCC Al-Co-Cr-Fe-Ni alloys. Metall Mater Trans A. 2020;51(6):3142–3153.
[16] Mehta A, Sohn YH. High entropy and sluggish diffusion 'core' effects in senary FCC Al–Co–Cr–Fe–Ni–Mn alloys. ACS Comb Sci. 2020;22(12):757–767.
[17] Dąbrowa J, Zajusz M, Kucza W, et al. Demystifying the sluggish diffusion effect in high entropy alloys. J Alloys Compd. 2019;783:193–207.
[18] Jin K,Zhang C, Zhang F, et al. Influence of compositional complexity on interdiffusion in Ni-containing concentrated solid-solution alloys. Mater Res Lett. 2018;6(5):293–299.
[19] Li Q, Chen W, Zhong J, et al. On sluggish diffusion in FCC Al–Co–Cr–Fe–Ni high-entropy alloys: an experimental and numerical study. Met (Basel). 2018;8(1):16.
[20] Mehta A. Fundamental core effects in Co-Cr-Fe-Ni based high entropy alloys. 2019; Electronic theses and dissertations (6333): https://stars.library.ucf.edu/etd/6333.
[21] Wang R, Chen W, Zhong J, et al. Experimental and numerical studies on the sluggish diffusion in face centered cubic Co-Cr-Cu-Fe-Ni high-entropy alloys. J Mater Sci Technol. 2018;34(10):1791–1798.
[22] Chen S, Li Q, Zhong J, et al. On diffusion behaviors in face centered cubic phase of Al-Co-Cr-Fe-Ni-Ti high-entropy superalloys. J Alloys Compd. 2019;791:255–264.
[23] Divinski SV, Pokoev AV, Esakkiraja N, et al. A mystery of 'sluggish diffusion' in high-entropy alloys: the truth or a myth? Diffus Found. 2018;17:69–104.

[24] Dąbrowa J, Danielewski M. State-of-the-art diffusion studies in the high entropy alloys. Met (Basel). 2020;10(3):347.
[25] Dayananda MA, Sohn YH. Average effective interdiffusion coefficients and their applications for isothermal multicomponent diffusion couples. Scr Mater. 1996;35(6):683–688.
[26] Belova IV, Sohn YH, Murch GE. Measurement of tracer diffusion coefficients in an interdiffusion context for multicomponent alloys. Philos Mag Lett. 2015;95(8):416–424.
[27] Schulz EA, Mehta A, Belova IV, et al. Simultaneous measurement of isotope-free tracer diffusion coefficients and interdiffusion coefficients in the Cu-Ni system. J Phase Equilib Diffus. 2018;39(6):862–869.
[28] Mehta A, Dickson J, Newell R, et al. Interdiffusion and reaction between Al and Zr in the temperature range of 425 to 475°C. J Phase Equilib Diffus. 2019;40(4):482–494.
[29] Mehta A, Zhou L, Keiser DD, et al. Anomalous growth of Al_8Mo_3 phase during interdiffusion and reaction between Al and Mo. J Nucl Mater. 2020;539(152337.
[30] Park Y, Newell R, Mehta A, et al. Interdiffusion and reaction between U and Zr. J Nucl Mater. 2018;502:42–50.
[31] Schulz E, Mehta A, Park SH, et al. Effects of marker size and distribution on the development of Kirkendall voids, and coefficients of interdiffusion and intrinsic diffusion. J Phase Equilib Diffus. 2019;40:156–169.
[32] Mehta A, Zhou L, Schulz EA, et al. Microstructural characterization of AA6061 versus AA6061 HIP bonded cladding–cladding interface. J Phase Equilib Diffus. 2018;39(2):246–254.
[33] Zhou L, Mehta A, Cho K, et al. Composition-dependent interdiffusion coefficient, reduced elastic modulus and hardness in γ-, γ'-and β-phases in the Ni-Al system. J Alloys Compd. 2017;727:153–162.
[34] Bronfin M, Bulatov G, Drugova I. Self-diffusion of Ni in the intermetallic compound Ni_3Al and pure Ni. Fiz Met Metalloved. 1975;40(2):363–366.
[35] Million B, Růžičková J, Velíšek J, et al. Diffusion processes in the Fe-Ni system. Mater Sci Eng. 1981;50(1):43–52.
[36] Rothman S, Nowicki L, Murch G. Self-diffusion in austenitic Fe-Cr-Ni alloys. J Phys F Met Phys. 1980;10(3):383.
[37] He Q, Ye Y, Yang Y. Formation of random solid solution in multicomponent alloys: from Hume-Rothery rules to entropic stabilization. J Phase Equilib Diffus. 2017;38:416–425.
[38] Bakker H. Enthalpies in alloys, Miedema's semi-empirical model. Enfield Publishing & Distribution Company; 1998, Enfield (NH) United States.
[39] Zhao S, Egami T, Stocks GM, et al. Effect of d electrons on defect properties in equiatomic NiCoCr and NiCoFeCr concentrated solid solution alloys. Phys Rev Mater. 2018;2(1):013602.